 CMES, vol.40, no.1, pp.63-81, 2009

Large-Scale Full Wave Analysis of Electromagnetic Field by Hierarchical Domain Decomposition Method

A. Takei[1], **S. Yoshimura**[1] **and H. Kanayama**[2]

Abstract: This paper describes a large-scale finite element analysis (FEA) for a high-frequency electromagnetic field of Maxwell equations including the displacement current. A stationary Helmholtz equation for the high-frequency electromagnetic field analysis is solved by considering an electric field and an electric scalar potential as unknown functions. To speed up the analysis, the hierarchical domain decomposition method (HDDM) is employed as a parallel solver. In this study, the Parent-Only type (Parallel processor mode: P-mode) of the HDDM is employed. In the P-mode, Parent processors perform the entire FEA. In this mode, all CPUs can be used without idling in an environment of 10-20 CPUs. A whole body cavity resonator (TEAM Workshop problem 29) and a real-world commuter train model with 12.8 million degrees-of-freedom are solved to verify accuracy and performance of the developed method.

Keywords: High-frequency electromagnetic field, Helmholtz equations, Finite element method, Hierarchical domain decomposition method

1 Introduction

In electronic device design, electromagnetic environment analyses considering Electro-Magnetic Interference (EMI) become increasingly important. In particular, research and development of high-frequency electromagnetic field analysis techniques is especially demanded. One technique used is the Finite Difference Time Domain (FDTD) method, in which simulations can be intuitively performed by discretizing the physical expression of electromagnetic wave propagation within Yee's grid [Luebbers, R.J. and Langdon, H.S. (1996)] [Anzaldi, G. and Silva, F. et al. (2007)]. However, when a detailed calculation model is created based on an actual living environment, its calculation scale becomes prohibitively large. On the other hand, the finite element method (FEM), in which an unstructured grid assures bound-

[1] The University of Tokyo, Bunkyo-ku, Tokyo, Japan
[2] Kyushu University, Nishi-ku, Fukuoka, Japan

ary conformity efficiently, is regarded desirable [Fujitsu Ltd. Poynting homepage]. The finite element method has been used to solve the Helmholtz equations in high-frequency electromagnetic problems, resulting in solving large-scale systems of simultaneous linear equations [Vouvakis, N.M. and Lee, J.F. (2004)] [Bertazzi, F. and Cappelluti, F. et al. (2006)] [Bleszynski, E. and Bleszynski, M. et al. (2004)]. It is also a crucial problem how to solve such large scale systems of equations derived from finite element discretization of the Helmholtz equations in high-frequency electromagnetic problems. It is known that the convergence of the Incomplete Cholesky Conjugate Orthogonal Conjugate Gradient (ICCOCG) method becomes worse as the size of the system increases. There have been efforts to improve the robustness of iterative solution methods in large-scale parallel analyses of electromagnetic environment problems requiring a complicated domain [Bielak, J., Ghattas, O. et al. (2005)] [Okamoto, M. and Himeno, R. et al. (2007)] [Takei, A. and Yoshimura, S., Kanayama, H. (2008)].

Currently, we are conducting a research on large-scale finite element analyses for problems using more than 10 million complex DOFs (degrees of freedom). In this study, we solve high-frequency electromagnetic fields in the range of several MHz to several GHz by using parallelization techniques based on the hierarchical domain decomposition method (HDDM). The HDDM has been successfully applied to solve elastic problems of approximately 100 million DOFs.

In this research, the equations to be solved are formulated according to the E Method, which takes the electric field $\mathbf{E}$ as an unknown function, and according to the E-ϕ Method, which takes the electric field $\mathbf{E}$ and the scalar potential ϕ as unknown functions. We reported the numerical examples of about 5.2 million complex DOFs by the E Method with the additional term until now [Takei, A. and Yoshimura, S., Kanayama, H. (2008)]. The iterative domain decomposition method based on the Conjugate Orthogonal Conjugate Gradient (COCG) method is applied to solve the interface problem. In a low-frequency eddy current problem, it has been shown that the computational time of an interface problem is reduced by the A-ϕ Method, which introduces the scalar potential ϕ into the A Method as an unknown function [Kanayama, H. and Sugimoto, S. (2006)]. The reentrant type whole cavity resonator model based on TEAM (Testing Electromagnetic Analysis Methods) workshop problem 29, one of the standard problems in numerical electromagnetic field analyses, is employed for assessing both accuracy and performance of our proposed method. To verify the accuracy of the developed method, we compare the calculated value with an actual measurement as well as the value calculated by the FDTD method. In addition, we compare the E method and the E-ϕ Method to discuss the effects on computational time and memory size. In these analyses, we employ two models with approximately 6 million and 12 million complex DOFs,

respectively. To the best of our knowledge, there has been currently no published result such that the scalar potential ϕ is considered in large-scale high-frequency electromagnetic field problems with more than 10 million complex DOFs.

2 Finite element formulation

2.1 E Method

Let Ω be a domain with the boundary $\partial\Omega$. The Helmholtz equation which describes an electromagnetic field with single angular frequency ω [rad/s] is drawn from Maxwell's equations containing the displacement current [Lu, Y.Y. and Zhu, J. (2007)] [Soares Jr, D. and Vinagre, M.P. (2008)] [Young, D.L. and Ruan, J.W. (2005)] [Reitich, F. and Tamma, K.K. (2004)]. The Helmholtz equations describing an electric field $\mathbf{E}$ [V/m] are given by (1a) and (1b) below, using the current density $\mathbf{J}$ [A/m^2] and the electric field $\mathbf{E}$**,** and assigning j as an imaginary unit:

$$rot\,(1/\mu rot\mathbf{E}) - \omega^2\varepsilon\mathbf{E} = j\omega\mathbf{J} \quad \text{in } \Omega \tag{1}$$

$$\mathbf{E}\times\mathbf{n} = \mathbf{0} \quad \text{on } \partial\,\Omega \tag{2}$$

$$\mathbf{J} = \sigma\hat{\mathbf{E}} \tag{3}$$

Permittivity and permeability are given by $\varepsilon = \varepsilon_0\varepsilon_r$ and $\mu = \mu_0\mu_r$, respectively. Here, ε_0 and $\mu_0$are the vacuum permittivity [F/m] and permeability [H/m], and ε_r and μ_r are the relative permittivity and permeability, respectively. In this formulation, permittivity becomes complex permittivity $\varepsilon = \varepsilon_0\varepsilon_r = \varepsilon_0\varepsilon_r' + \sigma/j$ [Chen, R.S. and Ping, X.W. et al. (2006)].

The electric field $\hat{\mathbf{E}}$ on known points is substituted into (1a) by equation (1c), where the electrical conductivity is denoted as σ. By solving equation (1a), with imposing the boundary condition of (1b), we calculate the electric field $\mathbf{E}$. The magnetic field $\mathbf{H}$ is then calculated from the electric field $\mathbf{E}$ by post-processing using equation (2) bellow, which is one of Maxwell's equations.

$$\mathrm{rot}\mathbf{E} - j\omega\mu_0\mu_r\mathbf{H} = \mathbf{0} \tag{4}$$

Finally, we assume that

$$\mathrm{div}\mathbf{J} = 0 \quad \text{in } \Omega \tag{5}$$

Next, we describe the finite element descritization. The electric field $\mathbf{E}$ is approximated with Nedelec elements (edge elements) [Golias, N.A. and Antonopoulos, C.S. et al. (1998)]. The finite element approximation is performed as follows

[Kanayama, H. and Tagami, D. et al. (2000)] [Kanayama, H. and Shioya, R. et al. (2002)] [Taeyoung, H. and Sangwon S. et al. (2006)] [Soares Jr., D. (2008)].

Find $\mathbf{E}_h$ such that

$$(1/\mu \mathrm{rot}\mathbf{E}_h, \mathrm{rot}\mathbf{E}_h^*) - \omega^2 (\varepsilon \mathbf{E}_h, \mathbf{E}_h^*) = j\omega (\mathbf{J}_h, \mathbf{E}_h^*) \tag{6}$$

where (,) denotes the complex valued L^2-inner product. Here, $\mathbf{J}_h$is a corrected electric current density with consideration of the continuity [Kanayama, H. and Sugimoto, S. (2006)].

2.2 *E-ϕ Method*

The scalar potential ϕ is introduced as an unknown function to the E Method described in the previous section. The Helmholtz theorem shown in equation (5) splits the vector field into the sum of the curl and gradient vectors as follows:

$$\mathbf{E} = \mathbf{E}_1 + \mathbf{E}_2 \tag{7}$$

$$\mathrm{div}\mathbf{E}_1 = 0 \tag{8}$$

$$\mathrm{rot}\mathbf{E}_2 = \mathbf{0} \tag{9}$$

$$\mathbf{E}_2 = -\mathrm{grad}\phi \tag{10}$$

where $\mathbf{E}_1$ and $\mathbf{E}_2$ represent the curl and gradient parts of the electric field $\mathbf{E}$, respectively. Equation (5) is substituted into equation (1a). Equation (6a) is then obtained by rewriting $\mathbf{E}_1$ to $\mathbf{E}$.

$$rot\,(1/\mu rot\mathbf{E}) - \omega^2 \varepsilon (\mathbf{E} - \mathrm{grad}\phi) = j\omega\mathbf{J} \quad \text{in } \Omega \tag{11}$$

$$div\left\{\omega^2 \varepsilon (\mathbf{E} - \mathrm{grad}\phi)\right\} = 0 \quad \text{in } \Omega \tag{12}$$

$$\mathbf{E} \times \mathbf{n} = \mathbf{0}, \quad \text{on } \partial\Omega \tag{13}$$

$$\mathbf{J} = \sigma\hat{\mathbf{E}} \tag{14}$$

Equation (6b) is obtained by taking the divergence of (6a). Let complex permittivity ε, permeability μ, and angle frequency ω be known parameters, as in the E Method. The electric field $\mathbf{E}$ and the scalar potential ϕ are calculated by the finite element analysis with (6c) and (6d). The scalar potential ϕ is approximated with first-order tetrahedral elements. The finite element approximation is as follows.

Find $\mathbf{E}_h$ and ϕ_h such that

$$(1/\mu \mathrm{rot}\mathbf{E}_h, \mathrm{rot}\mathbf{E}_h^*) - \omega^2 (\varepsilon \mathbf{E}_h, \mathbf{E}_h^*) + \omega^2 (\varepsilon \mathrm{grad}\phi_h, \mathbf{E}_h^*) = j\omega (\mathbf{J}_h, \mathbf{E}_h^*) \tag{15}$$

$$\omega^2(\varepsilon \mathbf{E}_h, \mathrm{grad}\phi_h^*) - \omega^2(\varepsilon \mathrm{grad}\phi_h, \mathrm{grad}\phi_h^*) = 0 \tag{16}$$

These formulations based on Maxwell's equations contain the displacement current, which cannot be disregarded in high-frequency electromagnetic field analysis. The electric field **E**, which is not usually considered in conventional eddy current analysis, is also calculated.

3 Algorithm for parallel computing

3.1 Interface problem

Let us put the finite element equations of (4) or (7) in matrix form, as follows:

$$Ku = f \tag{17}$$

where K denotes the coefficient matrix, u the unknown vector, and f the known right-hand side. As shown in the following equation, the domain Ω is decomposed into N pieces so there is no overlap in the boundary between the subdomains. A single element makes the minimum possible unit.

$$\Omega = \bigcup_{i=1}^{N} \Omega^{(i)} \tag{18}$$

The domain Ω is partitioned into non-overlapping subdomains. Then the linear system (8) is rewritten as follows:

$$\begin{bmatrix} K_{II}^{(1)} & \cdots & 0 & K_{IB}^{(1)} R_B^{(1)^T} \\ 0 & \ddots & \vdots & \vdots \\ 0 & \cdots & K_{II}^{(N)} & K_{IB}^{(N)} R_B^{(N)^T} \\ R_B^{(1)} K_{IB}^{(1)^T} & \cdots & R_B^{(N)} K_{IB}^{(N)^T} & \sum_{i=1}^{N} R_B^{(i)} K_{BB}^{(i)} R_B^{(i)^T} \end{bmatrix} \begin{bmatrix} u_I^{(1)} \\ \vdots \\ u_I^{(N)} \\ u_B \end{bmatrix} = \begin{bmatrix} f_I^{(1)} \\ \vdots \\ f_I^{(N)} \\ f_B \end{bmatrix} \tag{19}$$

where subscripts I, B correspond to nodal points in the interior of the subdomains, on the interface boundary, respectively. Here, $R_B^{(i)^T}$ represents the internal DOFs $u_B^{(i)}$ of subdomain $\Omega^{(i)}$ about u_B. It is a 0-1 procession to restrict. Equations (11) and (12) are obtained from equation (10).

$$K_{II}^{(i)} u_I^{(i)} = f_I^{(i)} - K_{IB}^{(i)} u_B^{(i)} \quad i = 1, ..., N \tag{20}$$

$$\left\{ \sum_{i=1}^{N} R_B^{(i)} \left\{ K_{BB}^{(i)} - K_{IB}^{(i)^T} (K_{II}^{(i)})^{-1} K_{IB}^{(i)} \right\} R_B^{(i)^T} \right\} u_B = \sum_{i=1}^{N} R_B^{(i)} \left\{ f_B^{(i)} - K_{IB}^{(i)^T} (K_{II}^{(i)})^{-1} f_I^{(i)} \right\}$$

(21)

where $f_B^{(i)}$ is the right-hand side vector of the equation regarding u_B. Equation (12) represents the interface problem of enforcing the continuity between subdomains in the domain decomposition method. Here, $(K_{II}^{(i)})^{-1}$ is the inverse matrix of $K_{II}^{(i)}$. Next, (12) is rewritten as equation (13).

$$Su_B = g \tag{22}$$

where S is described as follows:

$$S = \sum_{i=1}^{N} R_B^{(i)} S^{(i)} R_B^{(i)T} \tag{23}$$

$$S^{(i)} = K_{BB}^{(i)} - K_{IB}^{(i)T} (K_{II}^{(i)})^{-1} K_{IB}^{(i)} \tag{24}$$

where subscripts S and $S^{(i)}$ are the Schur complement matrix and the local Schur complement matrix in subdomain $\Omega^{(i)}$, respectively.

3.2 Iterative domain decomposition method

The algorithm based on the COCG method is applied to solve the interface problem shown in equation (13), and the internal boundary DOF u_B is calculated first. Here, δ is a non-negative constant used for testing convergence, and $||\,||$ indicates the Euclidean norm. Because the construction of the Schur complement matrix S requires a very large amount of computation time, we replace it with sub-steps (a) and (b), which are executed in each COCG step. Although a dot product operation must be performed for both sub-steps, the overall computation time is greatly reduced.

Choose u_B^0 ;

$p^0 = r^0 = Su_B^0 - g$; $\cdots\cdots\cdots(a)$

for $n = 0,1,.....;$

$q^n = Sp^n$; $\cdots\cdots\cdots(b)$

$$\alpha^n = \frac{(r^n)^T r^n}{(p^n)^T q^n};$$

$$u_B^{n+1} = u_B^n - \alpha^n p^n;$$

$$r^{n+1} = r^n - \alpha^n q^n;$$

IF $\left\|r^{n+1}\right\| < \delta\left\|r^0\right\|$, break;

$$\beta^n = \frac{(r^{n+1})^T r^{n+1}}{(r^n)^T r^n};$$

$$p^{n+1} = r^{n+1} + \beta^n p^n;$$

end;

(a) In each subdomain

Compute $u_I^{(i)0}$ by

$$K_{II}^{(i)} u_I^{(i)0} = f_I^{(i)} - K_{IB}^{(i)} R_B^{(i)T} u_B^0;$$

$$r^{(i)0} = K_{IB}^{(i)T} u_I^{(i)0} + K_{BB}^{(i)} R_B^{(i)T} u_B^0 - f_B^{(i)};$$

$$p^0 = r^0 = \sum_{i=1}^{N} R_B^{(i)} r^{(i)0};$$

(b) In each subdomain

Compute $p_I^{(i)n}$ by

$$K_{II}^{(i)} p_I^{(i)n} = -K_{IB}^{(i)} R_B^{(i)T} p^n;$$

$$q^{(i)n} = K_{IB}^{(i)T} p_I^{(i)n} + K_{BB}^{(i)} R_B^{(i)T} p^n;$$

$$q^n = \sum_{i=1}^{N} R_B^{(i)} q^{(i)n};$$

Finally, the solution of a whole domain can be obtained by calculating each subdomain DOF $u_I^{(i)}$ from equation (11). The finite element calculations of (a), (b) and equation (11) can be performed on each subdomain independently.

4 Hierarchical domain decomposition method

The original analysis domain is first divided into parts, which are further decomposed into smaller domains called subdomains. This is called the hierarchical domain decomposition method (HDDM). This is one of the most efficient techniques for parallel computing. HDDM has some modes depending on roles of processors.

4.0.1 Hierarchical Processor Mode

In the hierarchical processor mode (H-mode) [Yoshimura, S. and Shioya, R. et al. (2002)], processors are classified into three groups: Grand Parent, Parent, and Child. One of the processors is assigned as Grand Parent, a few as Parent, and others as Child. The number of Parent processors is the same as that of the parts. The number of Child processors can be varied; and it affects parallel performance.

The role of Grand Parent is to organize all processor communications (i.e., message passing) that occur between all processors. Parents prepare mesh data, manage finite-element analysis (FEA) results, and coordinate COCG iterations, including the convergence decision for COCG iterations. Parents send data to Child processors, where FEA is performed in parallel. After the FEA is finished, Child processors send the results to the Parents. This computation is repeated until the COCG iterations converge.

4.0.2 Parallel Processor Mode

An original HDDM is explained in the previous section. However, because most communication time is spent between Parent processors and Child processors, the communication speed is important. Although computer performance has been improved by advances in network technology in recent years, a high-speed network is still expensive. Generally in PC clusters often used, network speed is a bottleneck degrading the processing performance of the CPU. Moreover, when parallel processing performance is considered, it is important to reduce an amount of communications as much as possible. Therefore, the Parent-only type (parallel processor mode [P-mode]) is more useful than the H-mode that uses all three groups [Kanayama, H. and Sugimoto, S. (2006)].

In the P-mode, only Parent processors perform the FEA, which in the H-mode is computed by Child processors. In the H-mode, although Parent processors store some of the subdomain analyses data and coordinate the COCG iterations as primary work, the idle time of the CPU increases because the Parent processors perform fewer computations. In contrast, in P-mode, all processors in the P-mode perform the FEA, and every CPU can be used without idleness in an environment with 10-20 CPUs. Thus, the P-mode is considered superior to the H-mode in an

aspect of performance. In the P-mode, the number of Parent processors should be equal to that of the parts.

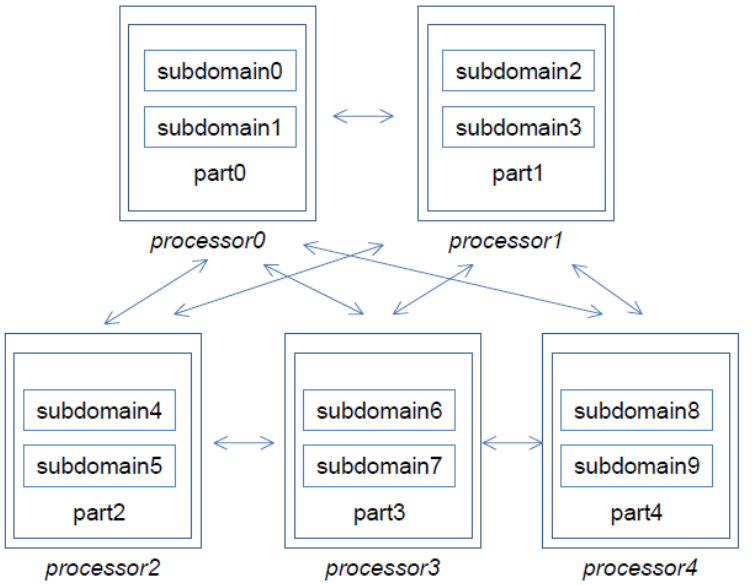

Figure 1: Data distribution and communication in the parallel processor mode.

5 Verification

5.1 Whole body cavity resonator

A reentrant resonator model is used to verify the accuracy and performance of the parallel computation, of our proposed method. The cavity is originally invented for hyperthermic cancer therapy. A disk-shaped lossy dielectric phantom is placed in the resonator cavity, then radio frequency electromagnetic energy is supplied. Because the resonant state must be maintained during a heating process, it is important to derive accurate resonant frequencies beforehand. To do so, the high-frequency electromagnetic problem must be solved. The cavity has a diameter of 1.90 [m] and a height of 1.45 [m]. In this analysis, the dielectric phantom of the shape of a disk with specific dielectric constant $\varepsilon_r = 80$ and electric conductivity $\sigma = 0.52$ [S/m] is placed, and the resonance state is investigated. This problem is one of the benchmark problems defined as TEAM Workshop Problem 29 [Kanai, Y. (1998)].

The analysis model is shown in Fig. 2 (a). The mesh, divided into first-order tetrahedral Nedelec elements, is shown in Fig. 2 (b). Verification is performed on

three kinds of meshes, described in Table 1. As in our previous work involving low-frequency eddy currents [Kanayama, H. and Sugimoto, S. (2006)], the highest calculation efficiency is achieved when the number of elements contained in one subdomain is about 100, and the number of partial domains is determined as such as that the number of elements contained in one subdomain be equal to 100.

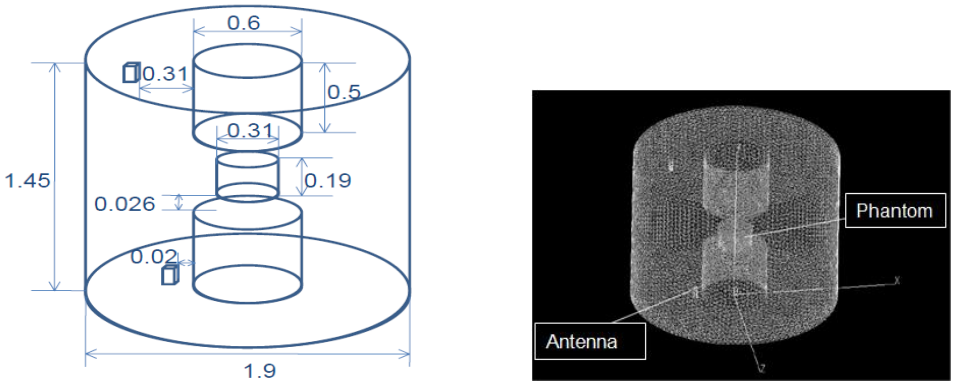

(a) Sketch of the model (unit: m) (b) Mesh

Figure 2: TEAM Workshop Problem 29.

Table 1: Meshes for verification.

	No. of Elements	DOFs	No. of Subdomains
Mesh (1)	108,787	134,889	36 x 302
Mesh (2)	4,528,311	6,108,779	36 x 1,258
Mesh (3)	10,073,267	13,515,847	36 x 2,798

5.2 Accuracy verification in frequency response analysis

Accuracy verification is performed using Mesh (1). To detect the resonant frequency and to compare solutions with actual measurements, the resonance state is investigated. The frequency band of 60 [MHz]-140 [MHz] is calculated for 2 [MHz] steps, and the response for every frequency step is investigated. Additionally, calculations near the resonance frequency are performed in 0.4 [MHz] intervals. All calculations are performed on an 18-node (36-core) PC cluster with Core2Duo 1.86 GHz processors and 2 GB RAM. The average CPU time per 1 frequency step and the average memory requirements are shown in Table 2. As for the E Method, the average CPU time per 1 step is 0.21 [h], and the CPU time solving

all 73 steps is 14.6 [h]. As for the E-ϕ Method, the average CPU time per 1 step is 0.18 [h], and the CPU time solving all 73 steps is 13.4 [h]. By using the E-ϕ Method, the CPU time is reduced by 11.5% compared to that using the E Method. The effect of the shortened CPU time by the introduction of the scalar potential ϕ is similar to the result previously reported for the A-ϕ Method [Kanayama, H. and Sugimoto, S. (2006)]. Moreover, compared with the E Method, the number of DOFs for the E-ϕ Method increases by more than 10%, and the memory usage also increases by more than 10%. However, since is far smaller than the total memory available on the cluster, it is not an obstacle in calculations.

Table 2: Average of CPU time and memory requirements.

	Formula -tion	DOFs	CPU time [h]	Memory size [Mbyte]
Mesh (1)	E	114,649	0.21	73.7
	E-ϕ	134,889	0.18	88.2

The frequency responses of the magnetic field by the E Method and the E-ϕ Method are shown in Fig. 3 (a) and (b), respectively. A comparison between the measured resonant frequencies and the solutions obtained by the FDTD method in each mode is shown in Table 3. The solution of the E Method and the E-ϕ Method are exactly the same as each other for each mode. The maximum error rate between the obtained solution and the measurement is 4.96% in the 1st mode. As the mode becomes higher, the error rate decreases. The same tendency is shown in the comparison of the error rate with solution of the FDTD method. Therefore, it is proved that the solution obtained by the proposed method has sufficiently high accuracy.

Table 3: Comparison of resonant frequencies in MHz. (Units: [MHz]. Error rate between measured data and numerical solution is shown in () [%].)

Resonance mode	Measured data	FDTD 25-mm mesh	E Result	E-ϕ Result
1st	68.6	67 (2.33)	65.2 (4.96)	65.2 (4.96)
2nd	110	110	109 (0.91)	109 (0.91)
3rd	134	134	134	134

5.3 Performance verification by large-scale model

Performance verification by large-scale computation using Mesh (2) and (3) is described next. In the analyses, the 1st mode (65.2 [MHz]) frequency is analyzed. Other calculation conditions are the same as those for Mesh (1). Average CPU

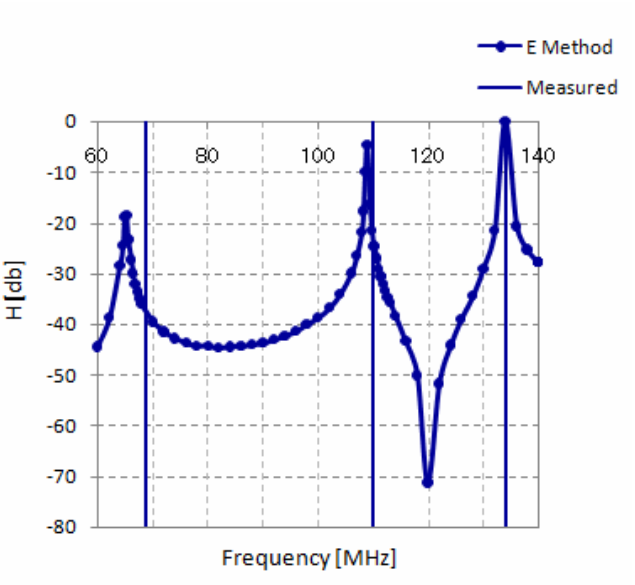

(a) Frequency response by the E Method

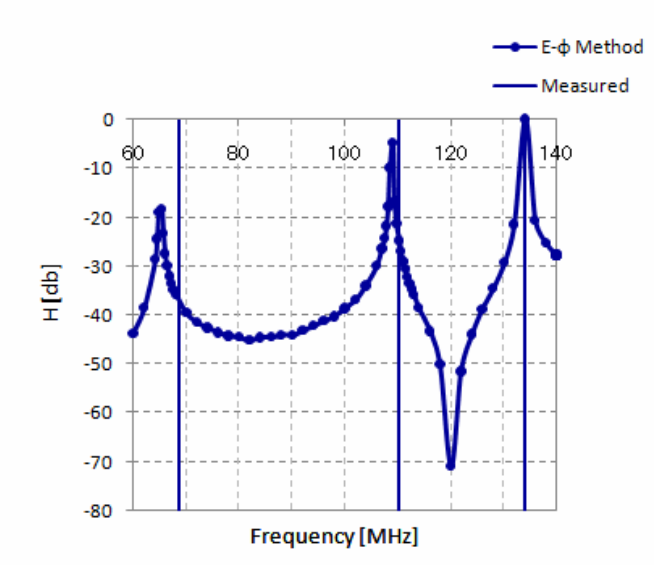

(b) Frequency response by the E-ϕ Method

Figure 3: Comparison of frequency responses of the E Method and the E-ϕ Method with measured data.

time and average memory requirements are shown in Table 4. For Mesh (2) solving with the E-ϕ Method, the CPU time is reduced by 11.5% as compared to that of the E Method. For Mesh (3), the E Method does not converge, but the E-ϕ Method successfully converges to compute a result. Although the E-ϕ Method uses approximately 10% more memory, the total amount used exceeds 25% of the available RAM, even for Mesh (3). Therefore, we do not consider memory usage to be a problem. The residual norm convergence history of COCG iterations in the interface problem is shown in Fig. 4. For the E Method, the number of iterations required until convergence is 5,865, whereas 4,685 iterations are required for the E-ϕ Method. In the calculations with Mesh (3), we can see the convergence behavior of the E Method. Here the interface problem does not converge even after 10,000 iterations. In contrast, by the E-ϕ Method, convergence is achieved after 4,556 iterations with a calculation time of 16.77 [h]. Those results confirm the superiority of the E-ϕ Method in large-scale computations. It is also demonstrated that the proposed method with the E-ϕ Method is able to solved high-frequency electromagnetic field problems of more than 10 million complex DOFs.

Table 4: CPU time and memory requirements for each mesh.

	Formulation	DOFs	CPU time [h]	Memory size [Mbyte]
Mesh (2)	E	5,355,008	7.43	1,860
	E-ϕ	6,108,799	6.44	2,100
Mesh (3)	E	11,857,646	-	-
	E-ϕ	13,515,847	16.77	8,244

5.4 Real-world application

To examine the applicability of the proposed method to in a real-world problem, we model the environment of a commuter train with four phantoms of human bodies inside. In such a commuter train, dielectrics such as phantoms and some plastic parts and metal parts exist. The electromagnetic field distribution may change due to differences of the geometric arrangement among these materials. Therefore, it is necessary to reproduce correctly a real environment. Some dielectrics such as plastic parts, and some reflective parts such as metals, which exist in a real commuter train, are modeled precisely in this numerical model [Monthly TRAIN (2004)]. The dimensions of the analysis model are shown in Figs. 5 (a) and (b). The CAD model is shown in Fig. 5 (c). The model has a length of 3.3 [m], a width of 3.4 [m], and a height of 3.25 [m]. A phantom is talking on a cellular phone. The electromagnetic field source is a cylinder type wave source imitating the cellular

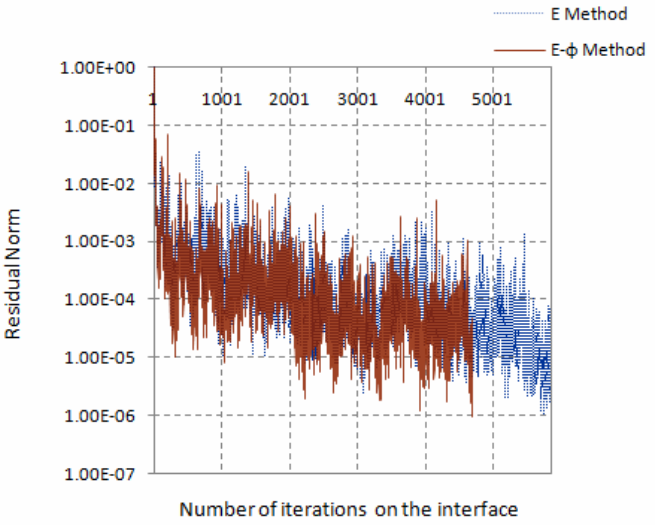

(a) Mesh (2)

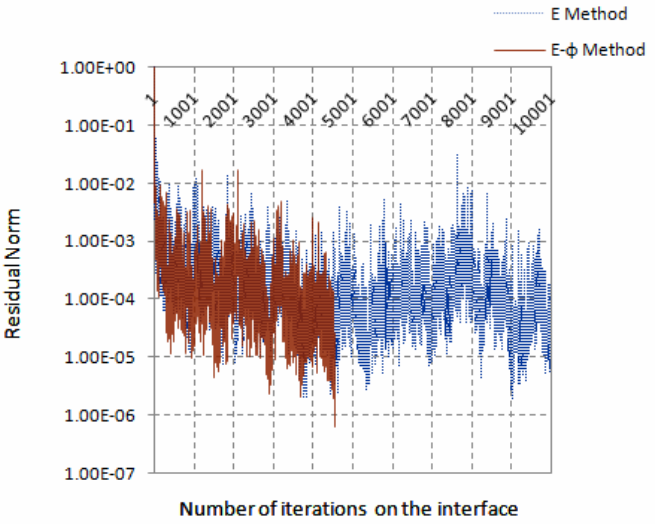

(b) Mesh (3)

Figure 4: Residual norm on the interface.

phone. In this analysis, the phantom composition is approximated by water, and the seats are considered to be plastic. The maximum size of the element edge length is 0.025 [m]. The number of complex DOFs is 12,869,405. The analysis frequency is set to be 300 [MHz].

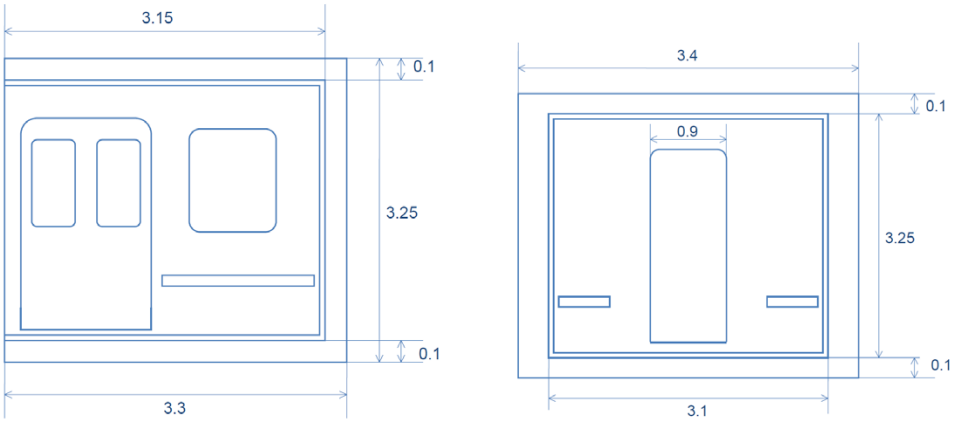

(a) Side view

(b) Cross section

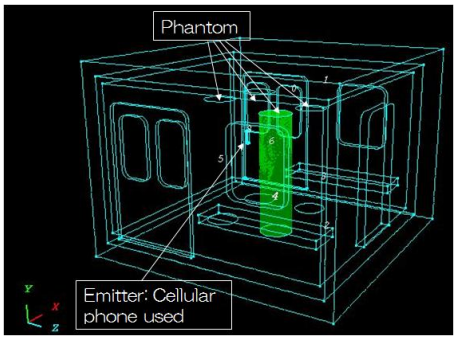

(c) CAD model.

Figure 5: Commuter train model (units: m).

The average CPU time and average memory requirements are shown in Table 5. The analyses do not converge when using the E Method as seriously as the numerical result in the report [Takei, A. and Yoshimura, S., Kanayama, H. (2008)]. By contrast, the analyses converge and complete the calculation when using the E-ϕ Method. The numerical solution (electric field intensity), visualized by ADVENTURE AutoGL [Kawai H. (2006)], is shown in Fig. 6. The mode of the electric field $\mathbf{E}$ in the commuter train is observed with a peak at the cellular phone circumference.

Table 5: Average of CPU time and memory requirements.

	Formula-tion	DOFs	CPU time [h]	Memory size [Mbyte]
Commuter train model	E	11,289,828	-	-
	E-ϕ	12,869,405	8.91	7,849

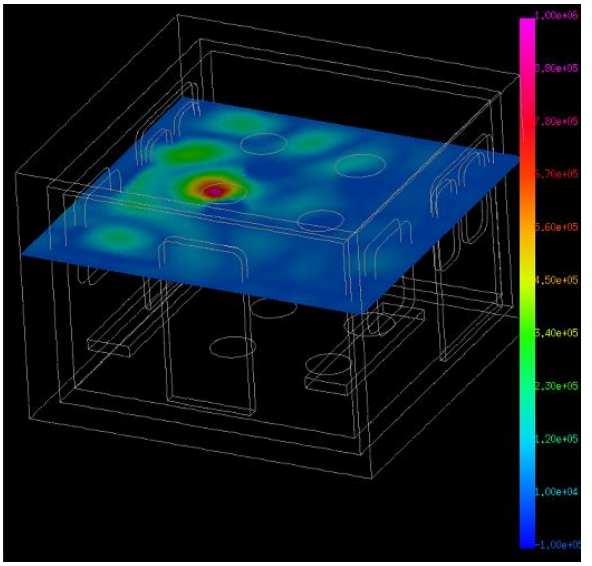

Figure 6: Electric fields in the commuter train.

6 Conclusions

In this paper, a large-scale finite element analysis techniques for high-frequency electromagnetic fields is newly proposed. Here, based on the hierarchical domain decomposition method (HDDM), the Helmholtz equation is discretized from Maxwell's equations of the frequency domain, including the displacement current.

Two kinds of formulations by the E Method and the E-ϕ Method are described and evaluated. The COCG method is employed to solve an interface problem in the HDDM.

Accuracy in frequency response analysis is verified by solving using the reentrant type whole cavity resonator model (TEAM Workshop Problem 29), and the performance is also verified by solving a large-scale analysis model. The values calcu-

lated by the E Method and the E-ϕ Method agree well each other, and also show good agreement with actual measurements and the numerical results obtained by the FDTD method. To assess performance in solving large scale problems, calculations for 6 million and 12 million complex DOF meshes are performed by both the E Method and the E-ϕ Method. When solving the problem with 6 million complex DOFs, the iterative calculation of the interface problem converges for both methods. However, as for the problem with 12 million complex DOFs, only the E-ϕ Method can converge and complete the calculation. This result shows that the E-ϕ Method is useful in large-scale problems.

We further confirm the effectiveness of our method with an environmental model of a real-world problem, i.e. a person making a cellular phone call in a commuter train. This high-frequency electromagnetic field analysis, at approximately 300 [MHz], is carried out using a large-scale numerical environmental model of approximately 12.8 million complex DOFs.

References

Anzaldi, G., Silva, F., Fernandez, M., Quiez, M., Riu, P.J. (2007): Initial Analysis of SAR From a Cell Phone Inside a Vehicle by Numerical Computation. *IEEE Trans. on Biomed. Eng.*, vol. 54, pp. 921-930.

Bertazzi, F., Cappelluti, F., Guerrieri, S.D., Bonani, F., Ghione, G. (2006): Self-Consistent Coupled Carrier Transport Full-Wave EM Analysis of Semiconductor Traveling-Wave Devices. *IEEE Trans. Microw. Theory Tech.*, vol. 54, pp.1611-1618.

Bielak, J., Ghattas, O., Kim, E.J. (2005): Parallel Octree-Based Finite Element Method for Large-Scale Earthquake Ground Motion Simulation. *CMES: Computer Modeling in Engineering & Sciences*, vol. 22, no. 3, pp. 235-248.

Bleszynski, E., Bleszynski, M., Jaroszewicz, T. (2004): Development of New Algorithms for High Frequency Electromagnetic Scattering. *CMES: Computer Modeling in Engineering & Sciences*, vol. 15, no. 2, pp. 295-318

Chen, R.S., Ping, X.W., Yung, E.K.N., Chan, C. H., Nie, Z., Hu, J. (2006): Application of Diagonally Perturbed Incomplete Factorization Preconditioned Conjugate Gradient Algorithms for Edge Finite-Element Analysis of Helmholtz Equations. *IEEE Trains. on Antennas and Propag.*, vol. 54, pp. 1604-1608.

Fujitsu Ltd. Poynting homepage, http://jp.fujitsu.com/solutions/plm/analysis/poynting/

Golias, N.A., Antonopoulos, C.S., Tsiboukis, T.D., Kriezis, E.E. (1998): 3D Eddy Current Computation with Edge Elements in Terms of the Electric Intensity. *International Journal for Computation and Mathematics in Electrical and Elec-*

tronic Engineering (COMPEL), vol. 17, pp. 667-673.

Kanai, Y. (1998): Description of TEAM Workshop Problem 29: Whole Body Cavity Resonator. *TEAM Workshop*, Tucson, AZ, USA.

Kanayama, H., Shioya, R., Tagami, D., Matsumoto, S. (2002): 3-D Eddy Current Computation for a Transformer Tank. *International Journal for Computation and Mathematics in Electrical and Electronic Engineering (COMPEL)*, vol. 21, pp. 554-562.

Kanayama, H., Sugimoto, S. (2006): Effectiveness of A-ϕ Method in a **Parallel Computing with an Iterative Domain Decomposition Method**. *IEEE Trans. Mag.*, vol. 42, pp. 539-542.

Kanayama, H., Tagami, D., Saito, M., Kikuchi, F. (2000): A Finite Element Analysis of 3-D Eddy Current Problems Using an Iterative Method. *Transactions of JSCES*, Paper no. 20000033, pp. 201-208.

Kawai, H. (2006): ADVENTURE AutoGL: A Handy Graphics and GUI Library for Researchers and Developers of Numerical Simulations. *CMES: Computer Modeling in Engineering & Sciences*, vol. 11, no. 3, pp. 111-120.

Lu, Y.Y., Zhu, J. (2007): Perfectly Matched Layer for Acoustic Waveguide Modeling - Benchmark Calculations and Perturbation Analysis. *CMES: Computer Modeling in Engineering & Sciences*, vol. 10, no. 2, pp. 99-112.

Luebbers, R.J., Langdon, H.S. (1996): A Simple Feed Model That Reduces Time Step Needed for FDTD Antenna and Microstrip Calculations. *IEEE Trans. Antennas Propag*., vol. 44, pp. 1000-1004.

Monthly TRAIN (2004), Eriei press, vol. 357. (in Japanese)

Okamoto, M., Himeno, R., Ushida, K., Ahagon, A., Fujiwara, K. (2007): The Coupled Analysis of Electromagnetic Wave and Heat Conduction with Rotational Motion of Heated Target and Temperature-Dependent Complex Permittivity. *T. IEEJ*, vol. 127-B, no. 8, pp. 902-910. (in Japanese)

Reitich, F., Tamma, K.K. (2004): State-of-the-art, Trends, and Directions in Computational Electromagnetics. *CMES: Computer Modeling in Engineering & Sciences*, vol. 5, no. 4, pp. 287-294.

Soares Jr., D. (2008): A Time-Domain FEM-BEM Iterative Coupling Algorithm to Numerically Model the Propagation of Electromagnetic Waves. *CMES: Computer Modeling in Engineering & Sciences*, vol. 32, no. 2, pp. 57-58.

Soares Jr., D., Vinagre, M.P. (2008): Numerical Computation of Electromagnetic Fields by the Time-Domain Boundary Element Method and the Complex Variable Method. *CMES: Computer Modeling in Engineering & Sciences,* vol. 25, no. 1, pp. 1-8.

Taeyoung, H., Sangwon, S., Dongwoo, S. (2006): Parallel Iterative Procedures for a Computational Electromagnetic Modeling Based on a Nonconforming Mixed Finite Element Method. *CMES: Computer Modeling in Engineering & Sciences*, vol. 14, no. 1, pp. 57-76.

Takei, A., Yoshimura, S., Kanayama, H. (2009): Large-scale Parallel Finite Element Analyses of High Frequency Electromagnetic Field in Commuter Trains. *CMES: Computer Modeling in Engineering & Sciences*, vol. 31, no. 1, pp. 13-24.

Vouvakis, N.M., Lee, J.F. (2004): A Fast Non-Conforming DP-FETI Domain Decomposition Method for the Solution of Large EM Problems. *In Proc. IEEE Int. Antennas and Propagation Symp.*, vol. 1, pp. 623-626.

Yoshimura, S., Shioya, R., Noguchi, H., Miyamura, T. (2002): Advanced General-purpose Computational Mechanics System for Large Scale Analysis and Design. *Journal of Computational and Applied Mathematics*, vol. 149, pp. 279-296.

Young, D.L., Ruan, J.W. (2005): Method of Fundamental Solutions for Scattering Problems of Electromagnetic Waves. *CMES: Computer Modeling in Engineering & Sciences*, vol. 7, no. 2, pp. 223-232.